Calcium Coordination and pH Dependence of the Calcium Affinity of Ligand-Binding Repeat CR7 from the LRP. Comparison with Related Domains from the LRP and the LDL Receptor†

Miljan Simonovic,‡,§ Klavs Dolmer,‡,§ Wen Huang,‡ Dudley K. Strickland,|| Karl Volz,▽ and Peter G. W. Gettins*,‡

Department of Biochemistry and Molecular Biology and Department of Microbiology and Immunology, College of Medicine, University of Illinois at Chicago, Chicago, Illinois 60612-4316, and American Red Cross, Rockville, Maryland

Received August 15, 2001; Revised Manuscript Received October 10, 2001

ABSTRACT: We have determined the X-ray crystal structure to 1.8 Å resolution of the Ca^{2+} complex of complement-like repeat 7 (CR7) from the low-density lipoprotein receptor-related protein (LRP) and characterized its calcium binding properties at pH 7.4 and 5. CR7 occurs in a region of the LRP that binds to the receptor-associated protein, RAP, and other protein ligands in a Ca^{2+}-dependent manner. The calcium coordination is identical to that found in LB5 and consists of carboxyls from three conserved aspartates and one conserved glutamate, and the backbone carbonyls of a tryptophan and another aspartate. The overall fold of CR7 is similar to those of CR3 and CR8 from the LRP and LB5 from the LDL receptor, though the low degree of sequence homology of residues not involved in calcium coordination or in disulfide formation results in a distinct pattern of surface residues for each domain, including CR7. The thermodynamic parameters for Ca^{2+} binding at both extracellular and endosomal pHs were determined by isothermal titration calorimetry for CR7 and for related complement-like repeats CR3, CR8, and LB5. Although the drop in pH resulted in a reduction in calcium affinity in each case, the changes were very variable in magnitude, being as low as a 2-fold reduction for CR3. This suggests that a pH-dependent change in calcium affinity alone cannot be responsible for the release of bound protein ligands from the LRP at the pH prevailing in the endosome, which in turn requires one or more other pH-dependent effects for regulating protein ligand release.

The low-density lipoprotein receptor-related protein (LRP)[1] is a member of the LDL receptor family of proteins (*1*). It is a 600 kDa multidomain, two-chain, membrane-anchored receptor that contains multiple copies of three different types of small repeated motifs. One of these motifs is an ∼40-residue domain that is related to a domain found in complement components 6 and 7 and that has consequently acquired the name complement-like repeat (CR). Complement-like repeats are present not only in all LDL receptor family members but also in other unrelated proteins such as enterokinase (*2*), transmembrane serine proteinase 2 (*3*), and the receptor for Rous sarcoma virus, Tva (*4*). At least in LDL receptor family members and in Tva, it is believed that these complement-like domains are responsible, either in whole or in part, for binding of target protein ligands. In the LRP and other LDL receptor proteins, complement-like repeats occur in clusters of different sizes. If one proceeds from the N-terminal end of the high-molecular mass α chain, the four clusters in the LRP contain 2, 8, 10, and 11 complement-like repeats, respectively. Of these four clusters, the second and fourth clusters appear to have the greatest range of ligand specificities and the highest affinities at physiological pH and hence are of the most functional interest (*5*).

The common features of the >1000 known complement-like domains are six almost completely conserved cysteines that form three disulfides, a cluster of four mostly conserved aspartate and glutamate residues in the C-terminal half of the domain that have been shown to be involved in calcium binding in the X-ray structure of LB5 from the LDL receptor (*6*), and three other residues (a phenylalanine, an isoleucine, and a serine). The remaining residues are variable, both in the type and in the length of the loops between disulfides in which they occur. Since each of these domains is relatively small, with little in the way of a hydrophobic core and hence with most of the side chains on the surface, this variability in loop length and composition is likely to result in unique surface topography and electrostatics for each such domain and require structures of each domain for a full understanding of individual ligand binding properties.

The nearly complete conservation among complement-like repeats of the residues shown in LB5 to be involved in calcium coordination, and the demonstration by NMR that cal-

† This work was supported by grant GMS4414 from the National Insitutes of Health (to P.G.W.G.).

* To who correspondence should be addressed. Phone: (312) 996-5534. Fax: (312) 413-0364. E-mail: pgettins@uic.edu.

‡ Department of Biochemistry and Molecular Biology, University of Illinois at Chicago.

§ These authors contributed equally to the study.

|| American Rd Cross.

▽ Department of Microbiology and Immunology, University of Illinois at Chicago.

[1] Abbreviations: LRP, low-density lipoprotein receptor-related protein; LDLR, low-density lipoprotein receptor; VLDLR, very low-density lipoprotein receptor; CR3, CR7, and CR8, third, seventh, and eighth complement-type repeats, respectively, from the LRP; GSH, reduced glutathione; GSSG, oxidized glutathione; ITC, isothermal titration calorimetry; LB1 and LB5, first and fifth complement-like repeats from the LDLR, respectively; TFA, trifluoroacetic acid.

10.1021/bi015688m CCC: $20.00
Published on Web 11/16/2001

	1			5					10						15					20				
CR3			-	Q	C	Q	P	G	E	F	A	C	A	N	S	-	R	C	I	Q	E	R	W	K	C
CR7	G	S	H	S	C	S	S	T	Q	F	K	C	-	N	S	G	R	C	I	P	E	H	W	T	C
CR8			G	G	C	H	T	D	E	F	Q	C	R	L	D	G	L	C	I	P	L	R	W	R	C
LB5			S	P	C	S	A	F	E	F	H	C	-	L	S	G	E	C	I	H	S	S	W	R	C
Consensus					C					F		C						C	I				**W**		C

	25				30				35					40							
CR3	D	G	D	N	D	C	L	D	N	S	D	E	A	P	A	L	C	H	Q		
CR7	D	G	D	N	D	C	G	D	Y	S	D	E	T	H	A	N	C	T	N	N	Q
CR8	D	G	D	T	D	C	M	D	S	S	D	E	K	S	-	-	C	E	G		
LB5	D	G	G	P	D	C	K	D	K	S	D	E	E	-	-	N	C	A	V		
Consensus	**D**	**G**			**D**	C		D		S	**D**	**E**					C				

FIGURE 1: Primary structures of the complement-like repeats (CR3, CR7, CR8, and LB5) examined in this study. The numbering given on top is that used for the new structure of CR7, starting with the N-terminal extension of GS introduced as part of the thrombin cleavage site used in protein purification as residues 1 and 2. The residues conserved between these four structures are shown at the bottom, and include five of the six calcium-coordinating residues. The sixth coordinating ligand is the carbonyl of Asp 27, which is also aspartate in CR3 and CR8, but is glycine in LB5.

cium binding causes a structuring of otherwise very flexible domains (*7*), has suggested that the known requirement of calcium for ligand binding to the LRP and other LDL receptor family proteins results from the ordering that occurs when calcium binds to these sites. On the basis of this model, it has been proposed that the lowered pH encountered by the endocytosed LRP−protein complexes when the vesicles fuse with endosomes causes ligand release as a result of calcium dissociation and loss of structure for the binding epitope (*6*, *8*).

As part of our long-term goal of understanding the basis for the wide range of protein specificity of the LRP and the mechanism of extracellular ligand binding and intracellular release, we are focusing on examining the structures and binding properties of complement-like repeats from cluster II of the LRP. We have previously used NMR spectroscopy to determine the solution structures of calcium complexes of CR3 and CR8 from the LRP (*9*, *10*) and to show that CR3 interacts with the receptor binding domain of α_2-macroglobulin (*10*). While NMR has the advantage of being a solution method, it has the limitation in this case of not being able to directly examine the calcium ion and its coordination. X-ray crystallography, however, can unambiguously provide details about metal coordination. We report here the X-ray crystal structure of a third complement-like domain from the LRP, CR7, as well as the calcium affinities of this and related domains, determined by isothermal titration calorimetry, at the pHs encountered both extracellularly and intracellularly after fusion with endosomes. We found the same calcium ion coordination in CR7 as in LB5, suggesting that this is likely to be invariant for other CR domains. Surprisingly, we found that, while there was always a reduction in calcium affinity for each of the complement repeats as the pH was reduced from that of the extracellular environment to that of the endosome, the affinities at pH 5 were all still too high to favor calcium dissociation as the mechanism for protein ligand release. An important conclusion is therefore that other pH-dependent factors must contribute in a major way to protein ligand release in the endosome.

MATERIALS AND METHODS

Expression, Purification, and Refolding of Complement-like Repeats. DNA fragments of the LRP and LDLR encoding single repeats were amplified from pcDNA 3.1-(LRP) and pLDLR-2 (ATCC, 39966) introducing a 5′ *Bam*HI site and a 3′ stop codon and *Eco*RI site using Expand (Roche). The fragments were inserted into pGEX-2T (Pharmacia) and expressed in *Escherichia coli* BL-21 cells as GST fusion proteins as previously described (*11*). After thrombin cleavage and GSH−Sepharose chromatography, the fragments were further purified to homogeneity by reverse phase HPLC on a semipreparative Vydac C18 column (10 mm × 250 mm), using a gradient of 10 to 60% acetonitrile in 0.1% TFA. The column was run at a flow rate of 4 mL/min, and elution was followed by absorption at 280 nm. Pooled fractions were freeze-dried. The denatured and reduced domains were folded by dilution into 50 mM Tris-HCl, 10 mM $CaCl_2$, 1 mM GSH, and 0.5 mM GSSG (pH 8.5) to a final concentration of <200 μg/mL, and dialysis against the latter buffer, as described previously (*7*). Refolded domains were purified by reverse phase HPLC as above. In all cases, the folded repeat eluted slightly earlier than the unfolded species. The sequences of the individual domains that were used, including any artificial linkers, are given in Figure 1.

Isothermal Titration Calorimetry. Calcium titrations were performed on a MicroCal MSC isothermal titration calorimeter. Experiments were performed at 30 °C. Buffers that were used were as follows: 20 mM Tris-HCl, 100 mM NaCl, and 0.02% NaN_3 (pH 7.4) and 20 mM sodium acetate, 100 mM NaCl, and 0.02% NaN_3 (pH 5.0). Proteins were diluted to 5 μM in buffer and were titrated with either 2 μL additions of 2 mM $CaCl_2$ in pH 7.4 buffer or 1 μL additions of 10 mM $CaCl_2$ in pH 5.0 buffer.

Isothermal titration calorimetry involves stepwise addition of an aliquot of titrant into a cell containing the binding species of interest. In the examples reported here, Ca^{2+} was titrated into complement-like repeats in the cell. The enthalpy of ligand binding is observed directly as heat that must be either added or removed from the reference cell to maintain a constant temperature. Thus, accurate measurements of ΔH can be obtained from such a titration as the sum of heats evolved to reach binding site saturation. Since the progress of the heat evolved or absorbed is also a measure of the degree of saturation of the ligand binding site, the same observable can be used as a reporter of binding, and hence serve for determination of K_d and thence of ΔG. The accuracy of the latter depends on the same consideration as

for any K_d determination, i.e., the protein concentration being within a range dictated by the K_d value to be measured.

Data were analyzed with the Origin software provided by the manufacturer. Fitting was done using a single-site model of binding, with the variables being the number of binding sites (n), K_d, and ΔH.

The relationships used in the data analysis are

$$K_d = (1 - \Theta)([X]/\Theta) \quad (1)$$

where Θ is the fraction of sites occupied by ligand X.

$$X_t = [X] + n\Theta M_t \quad (2)$$

where X_t and [X] are the total and free concentrations of ligand X, respectively, and M_t is the bulk concentration of the macromolecule in the cell.

$$Q = n\Theta M_t \Delta H V_0 \quad (3)$$

where Q is the total heat content of the solution in V_0 relative to the unliganded species and ΔH is the enthalpy of binding.

Taken together, these give a relationship for the heat evolved at any degree of saturation of

$$Q = (nM_t\Delta HV_0)/2[1 + X_t/nM_t + K_d/nM_t - \sqrt{(1 + X_t/nM_t + K_d/nM_t)^2 - (4X_t/nM_t)}] \quad (4)$$

For the ith injection, the heat released [$\Delta Q(i)$] is given by

$$\Delta Q(i) = Q(i) + dV_i/V_0[Q(i) + Q(i-1)]/2 - Q(i-1) \quad (5)$$

Using initial guesses for n, K_d, and ΔH (either entered directly or chosen by the program), the program calculates the ΔQ_i for each injection and compares the values with those determined experimentally. Improvements are made in n, ΔH, and K_d by standard Marquardt methods and comparison of theory and experiment. Iterations are continued until no further improvement in the fit is obtained.

Fluorescence Spectroscopy. Tryptophan fluorescence emission spectra of CR7 and other complement-like domains, as well as stimulated terbium emission spectra, were recorded on a PTI Quantamaster spectrofluorimeter, equipped with dual monochromators. Spectra were recorded using excitation at 280 nm and recording emission from 300 to 450 nm in the case of tryptophan emission spectra and from 300 to 555 nm for terbium emission spectra. Slits of 2 nm for excitation and 4 nm for emission were used. To obtain tryptophan emission spectra in the absence of calcium, 100 μM EDTA was added to the cuvette, whereas for spectra of the Ca^{2+} complex, 10 mM $CaCl_2$ was added.

X-ray Structure Determination. Crystals of the Ca^{2+}−CR7 complex were grown at 18 °C by the vapor diffusion hanging drop method and mixing equal volumes of the protein (6 mg/mL) and well solution [0.3 M NaCl and 20 mM sodium acetate (pH 3.8) containing 100 mM $CaCl_2$]. Crystals were serially transferred into buffer containing increasing concentrations of glycerol (from 5 to 20%) as a cryoprotectant and flash-frozen in liquid nitrogen. Diffraction data were collected at the temperature of liquid nitrogen on the BioCARS 14C bending magnet line at the Advanced Photon Source (Argonne National Laboratories, Argonne, IL) using a wavelength of 1.0 Å and a CCD-Q4 detector. A complete data set of 1° oscillations was recorded on a single crystal with approximate dimensions of 200 μm × 50 μm × 50 μm, using an exposure time of 40 s. The space group was $P2_12_12_1$, and the unit cell dimensions were as follows: a = 27.6 Å, b = 35.4 Å, and c = 36.3 Å. The high packing density resulted in 69% protein and 31% solvent in the crystal. One hundred thirty frames of data were indexed with DENZO (*12*) and scaled with SCALEPACK. The initial phases were determined by molecular replacement using the structures of LB5, CR3, and CR8 (PDB entries 1AJJ, 1D2L, and 1CR8, respectively). The search model did not contain either the extreme N-terminus (residues 1 and 2) or the C-terminus (residues 43 and 44). Molecular replacement calculations were performed with CNS (*13*). The oriented search model was then refined as a rigid body followed by cycles of simulated annealing to give an R_{cryst} of 39% (40−2.5 Å). Electron density maps were interpreted using the program Quanta. Ten percent of the data were randomly assigned to an R_{free} test for cross validation (*13*). The model was progressively refined using simulated annealing protocols, followed by energy minimization and manual inspection and rebuilding. Once the R-factor dropped below 35%, SHELX refinement protocols were used (*14*) and the resolution was increased stepwise to 2 Å. The final stages of refinement, including individual B-factor refinement, were carried out against all data in SHELX. The final model has an R-factor of 18.6% and an R_{free} of 22.2%. The crystallographic data and statistics are given in Table 1. Coordinates have been deposited with the Protein Data Bank (entry 1J8E).

Table 1: Data Collection and Refinement Statistics for CR7

crystal	
space group	$P2_12_12_1$
cell dimensions (Å)	a = 27.6, b = 35.4, c = 36.3
no. of crystals	1
data collection	
resolution limit (Å)	100−1.85
wavelength (Å)	1.00
no. of reflections (oberved/unique)	86028/2911
completeness (%) (overall/last shell)	88.5/56.6
R_{merge} (%) (overall/last shell)	7.2/26.8
$I/\sigma(I)$ (overall/last shell)	20/4
refinement	
no. of molecules in asymmetric unit	1
resolution used (Å)	40.00−1.80
effective resolution (Å)	1.85
average B-factor (Å^2)	21.0
no. of reflections (work/test)	2911/281
no. of protein atoms (amino acids)	332 (44)
no. of solvent molecules	31
no. of heterogen atoms	1
R_{cryst} ($\|F\| > 0\sigma$)	18.6
R_{free} ($\|F\| > 0\sigma$)	22.2
rms deviations from ideality	
bond lengths (Å)	0.005
bond angles (deg)	1.1

RESULTS

Crystal Structure of CR7. A stereorepresentation of the 1.8 Å resolution X-ray structure of the Ca^{2+}−CR7 complex is shown in Figure 2. All of the molecule, including the N-terminal tetrapeptide preceding the first cysteine and the C-terminal tetrapeptide following the last cysteine, is well-ordered in the final crystal structure (R_{cryst} = 18.6% and R_{free}

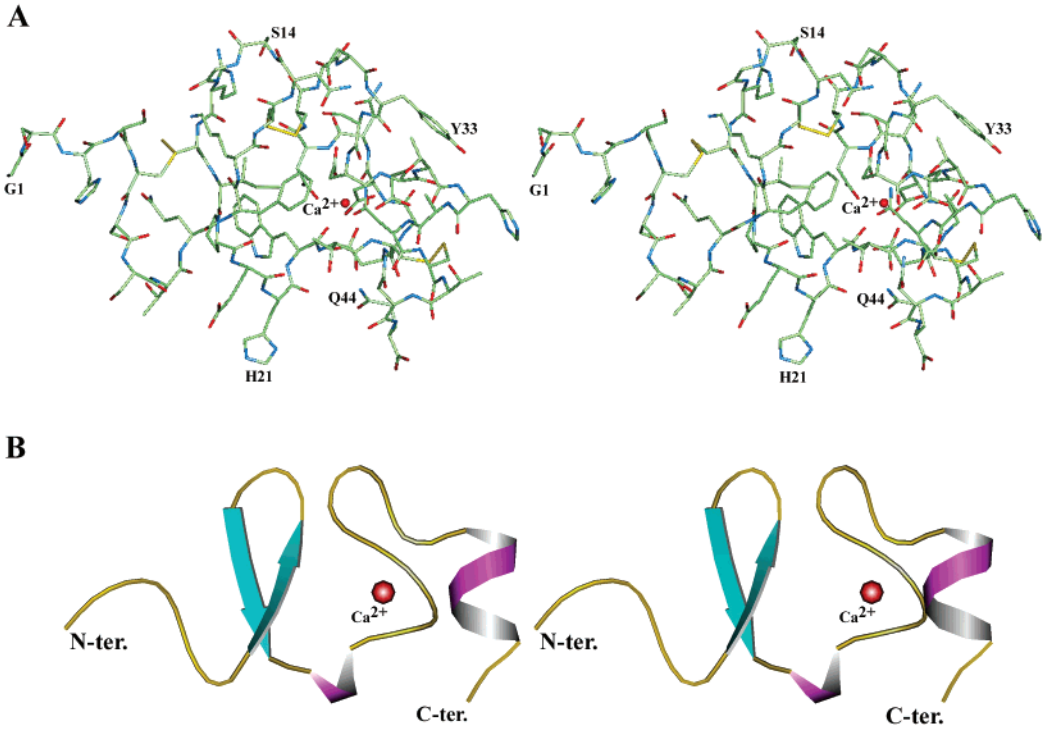

FIGURE 2: Stereorepresentations of the 1.8 Å crystal structure of the 44-residue CR7 domain from LRP. (A) Structure of CR7. All atoms are presented, with selected residues numbered and the calcium-binding site indicated. (B) Ribbon representation of CR7 in the same orientation as in panel A.

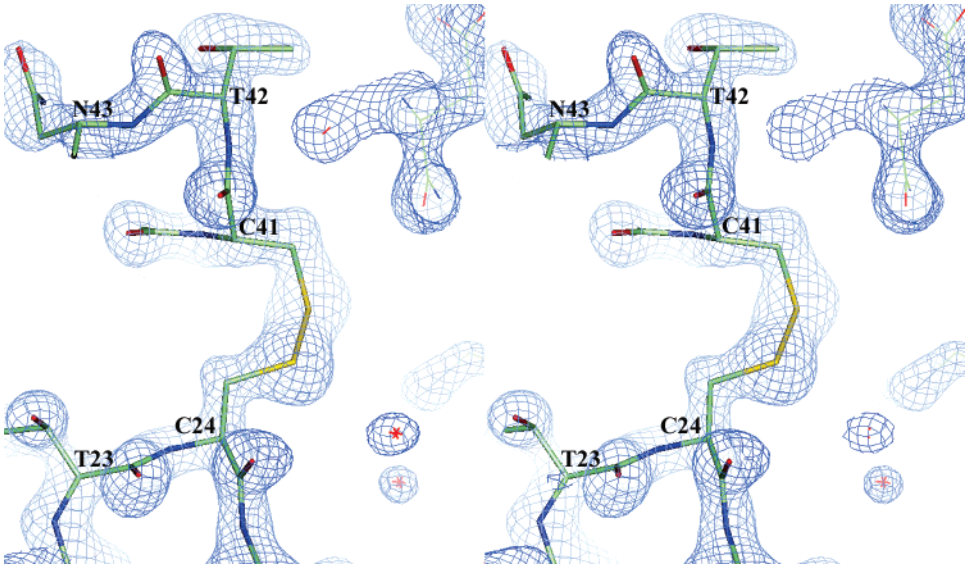

FIGURE 3: Stereoview of a representative $2|F_o - F_c|$ electron density map of the C-terminal part of CR7 showing the third disulfide between C24 and C41, contoured at 2σ.

= 22.4%; Table 1). Representative electron density is shown in Figure 3. As with structures of other complement-like repeats, the structure of CR7 is composed of an N-terminal lobe that contains a two-strand antiparallel mini β-sheet, here involving residues 9−11 and 16−18, and a C-terminal lobe that contains a one-turn α-helix, here involving residues 38−41. Each of the lobes also contains one disulfide. The two lobes are connected by a one-turn α-helix and by the third disulfide. A minimal hydrophobic core is composed of residues Phe 10 and Ile 18. Trp 22 does not contribute to this hydrophobic core, but instead has the indole side chain projecting outward into the solvent, as in other related structures. The calcium site is readily visible in the electron density map in the C-terminal lobe of the domain (Figure 4). Calcium coordination is octahedral and involves the carboxyl side chains of aspartates 25, 29, and 35 and of glutamate 36 and the backbone carbonyls of tryptophan 22 and aspartate 27. This geometry and coordination are identical to those found in the crystal structure of LB5 (*6*) and to those inferred for the NMR structures of CR3 and CR8 from the positions of the equivalent acidic side chains and the amide chemical shifts of residues immediately and C-terminally adjacent to the carbonyls involved in calcium coordination (*9*, *10*).

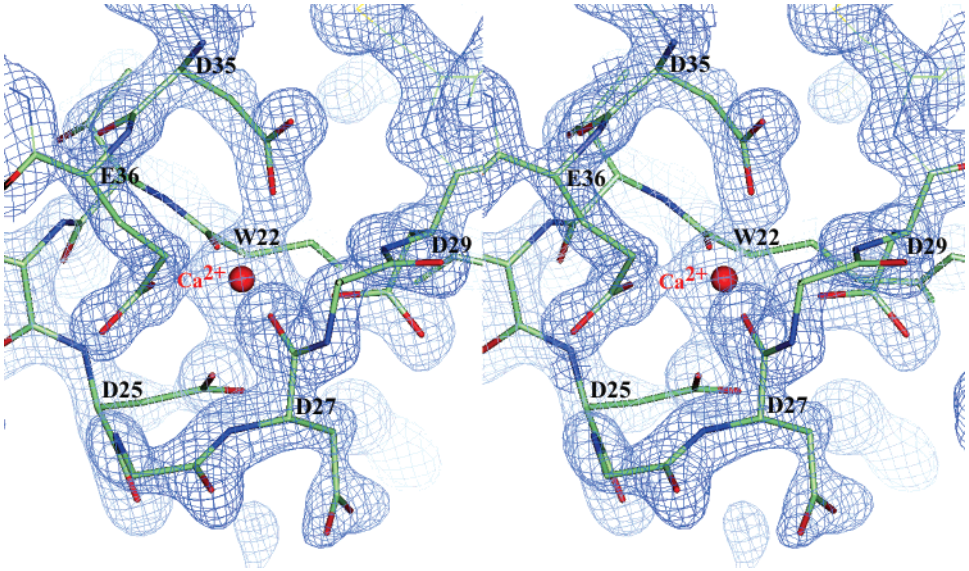

FIGURE 4: Stereorepresentation of the calcium binding site of CR7 showing the $2|F_o - F_c|$ electron density map and all atoms of the calcium-coordinating residues, contoured at 2σ.

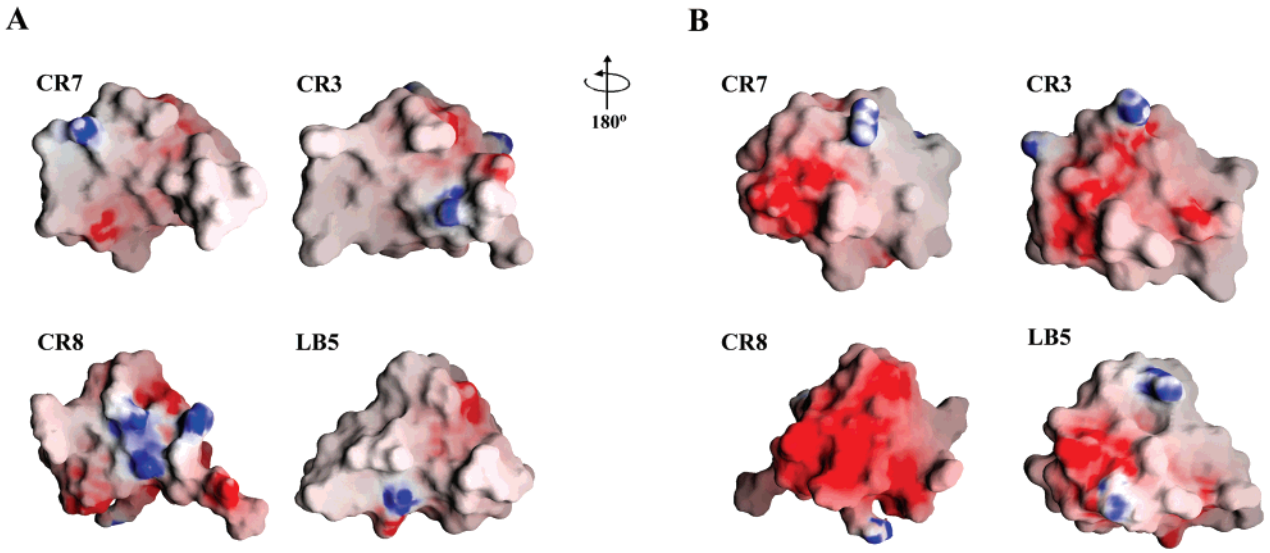

FIGURE 5: Comparison of the electrostatic surfaces of LRP domains CR3, CR7, and CR8 and domain LB5 from the LDLR represented by the program GRASP (*27*). (A) Same orientation as in Figure 2. (B) View after a 180° rotation about the vertical axis, as indicated. Regions of negative surface potential (less than $-15kT$) are shown in red, and regions of positive surface potential (greater than $15kT$) are shown in blue.

A comparison of the surface of CR7 with those of CR3, CR8, and LB5 reveals that each is quite distinct, with different numbers and distributions of charged and uncharged residues (Figure 5). For the presented structures, CR7 is most similar to CR3 and least similar to CR8. The face presented at right is that identified in a previous study for CR3 as the one that binds directly to the receptor binding domain of human α_2-macroglobulin. This face of CR7 is very different from that of CR8. Structural comparison of the backbones of CR7 with the backbones of CR3, CR8, and LB5 gave rmsds of 1.35, 1.53, and 1.13 Å, respectively, after making allowance for any insertions or deletions between the structures and comparing only residues between the first and last cysteines of each domain. Thus, of the LRP domains that were examined, CR7 most closely resembles LB5 in backbone structure.

Calcium Binding to Complement-like Domains. We used isothermal titration calorimetry (ITC) to determine the thermodynamics of binding of Ca^{2+} to single complement-like repeats CR3, CR7, and CR8 from the LRP, and LB5 from the LDL receptor. Measurements were taken at both pH 7.4 and 5.0. For all domains at both pH values, calcium binding was exothermic, with sufficiently large enough enthalpies of binding to give readily measured heat evolution for each injection of calcium and hence a good measure of the ΔH of binding (Figure 6). Since the K_d, and hence ΔG, could also be independently determined from fitting the experimental data to a binding curve, a complete thermodynamic analysis was possible for each binding process. The values presented (Table 2) are averages of three or more determinations, and the errors within each determination were between 4 and 25%.

At pH 7.4, calcium binds to each of the four single domains with similar ΔG values of $\sim 7.7 \pm 1$ kcal/mol. The domain with the highest affinity is LB5 with a K_d determined here of 0.5 μM. This is significantly weaker than that

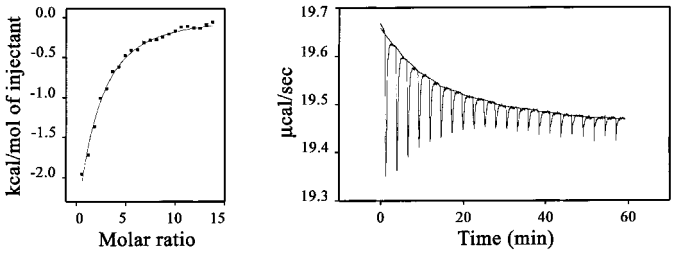

FIGURE 6: Representative raw ITC data for binding of calcium to CR7 (right) and a fitted binding isotherm (left) after correcting for the heat of dilution of calcium into buffer.

Table 2: Thermodynamics of Calcium Binding to Complement-like Repeats[a]

	pH 7.4					pH 5.0				
	K_d (μM)	ΔG^b	ΔH^b	$-T\Delta S^b$	ΔS^c	K_d (μM)	ΔG^b	ΔH^b	$-T\Delta S^b$	ΔS^c
CR3	8.0 ± 1.2	-7.1	-4.9 ± 0.3	-2.2	7.3	12.5 ± 1.1	-6.8	-6.3 ± 0.8	-0.4	1.4
CR7	12.6 ± 1.1	-6.8	-5.7 ± 0.3	-1.1	3.6	640 ± 160	-4.5	-7.7 ± 0.6	3.2	-10.6
CR8	6.1 ± 1.2	-7.2	-5.3 ± 0.8	-1.9	6.3	20.5 ± 5.2	-6.3	-3.5 ± 0.8	-3.0	10.0
LB5	0.5 ± 0.06	-8.7	-6.5 ± 1.5	-2.2	7.2	13.1 ± 2.3	-6.7	-2.3 ± 0.5	-4.4	14.5

[a] All titrations were carried out at least in triplicate. Values are the means $\pm$ half the range of the variation for the parameters determined directly. [b] In kilocalories per mole. [c] In calories per mole per kelvin.

reported from a titration followed by tryptophan fluorescence in the presence of EGTA as the competing ligand, which gave a value of 70 nM (*6*). Our value may, however, be an underestimate of affinity, given that the protein concentration needed for the ITC experiment was 5 μM and therefore too high to determine a K_d of <100 nM with good accuracy. The similarity of ΔH values may reflect the apparently identical calcium coordination sites in each domain. The much greater variation in ΔG results from differences in entropic contributions. Since calcium binding is responsible for structuring the whole domain, such variation in entropic contribution is perhaps not surprising and might depend on the primary structure and how many side chains became partially or wholly buried upon calcium-induced folding of the domain. No obvious correlation is apparent, however, between the calculated entropy change and the number of proline and glycine residues in particular domains.

At pH 5, all of the domains exhibited a reduction in affinity, though with large variations in both the relative changes and the resulting absolute affinities. CR7 and LB5 exhibited the largest relative changes in affinity. However, the source of the change was different in each case, resulting mainly from a change in enthalpy in the case of LB5, but of entropy in the case of CR7, which in fact offset a more favorable enthalpy change. This conclusion would not be altered if the previously published K_d of 70 nM were used for calcium binding to LB5 at pH 7.4 (*6*). The resulting affinities at pH 5.0 were also very different, being still quite high for LB5 ($K_d = 13\ \mu$M), but very much weaker for CR7 ($K_d = 640\ \mu$M). CR3 and CR8 exhibited much smaller reductions in affinity upon lowering the pH from 7.4 to 5.0. For CR3, the change was only a factor of 2, which resulted from nearly compensating changes in enthalpy (more favorable) and entropy (less favorable). For CR8, the situation was reversed, with a less favorable enthalpy of binding being partly compensated by a more favorable entropy change upon binding. It was surprising both that different factors (ΔH or ΔS) appeared to have different importance for the various domains and also that the final calcium affinity at pH 5 was still relatively tight for all domains except CR7.

Table 3: Fluorescence Properties of Complement-like Repeats, with Excitation at 280 nm

	without Ca^{2+}		with Ca^{2+}		Tb^{3+}
	intensity[a]	λ_{max} (nm)	intensity[a]	λ_{max} (nm)	intensity[b]
CR3	0.37	345	0.75	351	0.56
CR7	1.00	345	1.28	345	1.00
CR8	0.66	345	1.57	345	2.00
LB5	0.31	353	0.66	354	0.62

[a] Normalized to the intensity of the CR7 repeat in the absence of Ca^{2+} (1.00). [b] Normalized to the intensity of the CR7$-Tb^{3+}$ complex at 545 nm (1.00).

Fluorescence Emission Spectra of Complement-like Domains. We have previously found for repeats CR3 and CR8 from the LRP and for LB1 from the LDL receptor that the single tryptophan present in each of these repeats gave a fluorescence emission spectrum with a different intensity and different sensitivity to calcium binding (*7*). In addition, the proximity of the calcium site to the indole side chain resulted in sensitized terbium emission when Tb^{3+} was used as a replacement for Ca^{2+} and terbium was indirectly excited via irradiation of the tryptophan at 280 nm. To extend these observations to the new repeat CR7 and make comparisons with the only other domain for which the location of the calcium relative to the tryptophan is unambiguously known, LB5, we recorded both tryptophan emission spectra of these repeats in the absence and presence of calcium as well as the sensitized terbium emission spectra of the Tb^{3+} complexes.

At equivalent protein concentrations, CR7 gave the highest tryptophan fluorescence emission in the absence of calcium (Table 3). The relative intensities for the other three domains were 66% for CR8, 37% for CR3, and 31% for LB5. The wavelength maxima ranged from 353 nm for LB5 to 345 nm for the remainder. Upon binding calcium, CR7 exhibited the smallest relative enhancement, with a 28% increase. Each of the other domains gave enhancements of ~2-fold (Table 3). Only for CR3 was there a significant wavelength shift upon calcium binding (6 nm to the red). Each of the four domains gave efficient stimulated Tb^{3+} emission upon

excitation of the single tryptophan at 280 nm, reflecting the short separation between the metal ion and indole side chain. While the highest Tb^{3+} emission intensity was obtained from the domain with the highest tryptophan emission in the Ca^{2+}-bound state (CR8), the relationship between tryptophan and terbium fluorescence was not linear for the other domains (Table 3).

DISCUSSION

The extracellular binding of the many protein ligands to the LRP and related receptors, and the subsequent release of these ligands following endocytosis and recycling of the intact receptor to the cell surface, depends on the structures of the ligand-binding domains within the LRP, on the role and pH dependence of calcium in modulating the structure and ligand specificity of these domains, and possibly on other factors. In this study, we have used X-ray crystallography, isothermal titration calorimetry, and fluorescence to investigate the structure, calcium coordination, and pH dependence of calcium binding of ligand-binding domain CR7 from the LRP, and compared these properties with those of related domains from the LRP (domains CR3 and CR8) and the LDL receptor (domain LB5).

Unlike the previous two structures of ligand-binding domains from the LRP (CR3 and CR8), which were determined by NMR spectroscopy and therefore did not directly give the location and coordination of the bound calcium ion (*9*, *10*), our crystal structure of CR7 gives direct visualization of the calcium and its coordinating groups, a first for a domain from the LRP. Inspection of the primary structures of the 31 complement-like domains from the LRP shows that the glycine residue that was found to coordinate to calcium in the X-ray crystal structure of LB5 is instead mostly an aspartate in the LRP. This had suggested to us that the calcium coordination in LRP might differ from that of the LDLR by having an additional carboxylate side chain as a ligand in place of the carbonyl of the same residue. During NMR structure determinations of both CR3 and CR8, we found that there was little energy difference between structures that had the side chain carboxyl of this asparate coordinated to calcium and those that had the backbone carbonyl coordinated in the same way as in LB5. Nevertheless, we favored backbone carbonyl coordination of this aspartate in CR3 and CR8 based on the chemical shifts of the amide nitrogens of the adjacent residues. For CR7, we now have clear evidence for such carbonyl coordination by the additional aspartate residue and for the side chain to project into solution, where it is available for binding to protein ligands (Figure 4). The remaining calcium ligands are identical in the structures of LB5 and CR7. It is therefore likely that the >90% of complement-like repeats identified that contain the four conserved aspartates and glutamate (residues 25, 27, 29, 35, and 36 in CR7, Figure 1) bind calcium and adopt coordination identical to that found here for CR7 and earlier by others for LB5.

The crystal structure of CR7 revealed a backbone fold that is highly similar to those of complement-like repeats of known structure, specifically, CR3, CR8, and LB5 (*6*, *9*, *10*). Indeed, the ability to determine the structure of CR7 by molecular replacement, using a model based primarily on the structure of CR8, indicates the high degree of backbone structural similarity. This contrasts with the very high variation in primary structure among all complement-like domains beyond the conserved disulfides and calcium-coordinating side chains. Given this high degree of primary structure variation, it is perhaps not surprising that the surface of CR7 is very different from those of other complement-like domains. Having the structure of CR7 as the third such domain from the principal protein ligand-binding region of LRP will therefore be invaluable in determining and understanding interaction sites with different protein ligands.

As with other complement-like repeats we have examined, the single tryptophan, which is largely conserved, gives a fluorescence enhancement upon calcium binding and structural rigidification of the domain. However, in keeping with the highly variable primary structures of these complement-like repeats, and the consequent variability in residues of contact with this tryptophan, the tryptophan fluorescence intensity differs both in the absence and in the presence of calcium from that of other repeats. Similarly, the sensitized Tb^{3+} emission is different from that of other complement-like domains we have examined.

Perhaps the most important findings of this study are the surprisingly modest changes in affinities of Ca^{2+} for CR7 and related domains between pH 7.4 and 5.0. A previously proposed mechanism of ligand binding to and release from the LRP and other LDL receptor proteins involves extracellular binding of calcium to the LRP, where the free calcium concentration is in the millimolar range (*15*), and dissociation of calcium within the endosomes as a result of a lower calcium concentration in the 10 μM region and a reduced pH (*6*, *8*). Accordingly, we had expected to find very large reductions in calcium affinity upon reduction of the pH to that found intracellularly upon fusion of endocytosed LRP ligand-containing vesicles with endosomes. Such large reductions in affinity, with the consequent release of calcium, the loss of the structural integrity of the domains, and hence the loss of protein ligand affinity, would have provided a simple explanation for the pH-dependent binding and release of ligands from the LRP. Although CR7 itself does show an ~50-fold drop in calcium affinity, into the millimolar range, the other complement-like domains show either small relative affinity changes (CR3 and CR8) or a large change but with still tight final affinity at pH 5 (LB5). Since it is likely that the bound protein ligand will enhance the overall calcium affinity, the calcium affinities reported here for free domains are likely to be lower than for calcium in LRP−protein ligand complexes. Despite the active pumping of calcium out of endocytosed vesicles (*16*), the concentration of calcium is still ~10 μM after 5 min, which would probably result in most calcium binding sites on LRP−ligand complexes still being occupied. To account for the observed ligand dissociation, it is therefore necessary to invoke additional pH-dependent factors in overall ligand affinity. One possibility is the earliest suggestion of ionic interactions between basic residues on the ligand and acidic residues on the receptor. This would help to explain the critical role of positively charged side chains in ligands such as apoE (*17*) and α_2-macroglobulin (*18*, *19*), while still acknowledging a (lesser) role for weakened calcium affinity in promoting ligand dissociation. An additional, or alternative, explanation is that there is an allosteric pH-dependent effect of other domains of the LRP in promoting ligand dissociation at low pH.

Although such studies have not been carried out directly on the LRP, studies on the smaller but structurally related VLDL and LDL receptors have shown that deletion of the adjacent YWTD and EGF domains and the O-linked sugar domain results in the loss of the ability to release bound ligand, though not to internalize them (*20*, *21*). A recent X-ray stucture determination of the cluster of six YWTD domains from LDLR, together with their flanking EGF domains, shows that the YWTD domains form a propeller-like structure (*22*), as previously predicted (*23*), with the suggestion that pH-dependent unstructuring, possibly involving opening of the domain−domain contacts, could result in allosteric effects on bound ligands and their release at low pH (*22*, *24*).

A second role of calcium in promoting correct folding and disulfide bond formation of the complement-like repeats of the LRP and other LDL receptor family members may be equally or even more important. Indeed, it has been shown that mutation of calcium-coordinating residues results in misfolding in vitro (*25*) and may contribute to disease such as hypercholesterolemia in vivo (*26*). In this way, although Ca^{2+} may thus not be the principal determinant of protein ligand release or even an absolute requirement for protein ligand binding, it probably still plays a critical role in the functioning of the LRP and related members of the LDL receptor family.

ACKNOWLEDGMENT

We thank Drs. Brian K. Shoichet and Marty Watterson (Northwestern University, Evanston, IL) for making the isothermal titration calorimeter available to us and Dr. Tom Lucas for help with initial ITC experiments.

REFERENCES

1. Herz, J., Hamann, U., Rogne, S., Myklebost, O., Gausepohl, H., and Stanley, K. K. (1988) *EMBO J. 7*, 4119−4127.
2. Kitamoto, Y., Yuan, X., Wu, Q., McCourt, D. W., and Sadler, J. E. (1994) *Proc. Natl. Acad. Sci. U.S.A. 91*, 7588−7592.
3. Paoloni-Giacobino, A., Chen, H., Peitsch, M. C., Rossier, C., and Antonarakis, S. E. (1997) *Genomics 44*, 309−320.
4. Rong, L., and Bates, P. (1995) *J. Virol. 69*, 4847−4853.
5. Strickland, D. K., Kounnas, M. Z., and Argraves, W. S. (1995) *FASEB J. 9*, 890−898.
6. Fass, D., Blacklow, S., Kim, P. S., and Berger, J. M. (1997) *Nature 388*, 691−693.
7. Dolmer, K., Huang, W., and Gettins, P. G. W. (1998) *Biochemistry 37*, 17016−17023.
8. Brown, M. S., Herz, J., and Goldstein, J. L. (1997) *Nature 388*, 629−630.
9. Huang, W., Dolmer, K., and Gettins, P. G. W. (1999) *J. Biol. Chem. 274*, 14130−14136.
10. Dolmer, K., Huang, W., and Gettins, P. G. W. (2000) *J. Biol. Chem. 275*, 3264−3271.
11. Bieri, S., Djordjevic, J. T., Daly, N. L., Smith, R., and Kroon, P. A. (1995) *Biochemistry 34*, 13059−13065.
12. Otwinowski, Z., and Minor, W. (1997) *Methods Enzymol. 276*, 461−472.
13. Brünger, A. T. (1998) *Acta Crystallogr. D54*, 905−921.
14. Sheldrick, G. M., and Schneider, T. R. (1997) *Methods Enzymol. 277*, 319−343.
15. Carafoli, E. (1987) *Annu. Rev. Biochem. 56*, 395−433.
16. Gerasimenko, J. V., Tepikin, A. V., Petersen, O. H., and Gerasimenko, O. V. (1998) *Curr. Biol. 8*, 1335−1338.
17. Wilson, C., Wardell, M. R., Weisgraber, K. H., Mahley, R. W., and Agard, D. A. (1991) *Science 252*, 1817−1822.
18. Nielsen, K. L., Holtet, T. L., Etzerodt, M., Moestrup, S. K., Gliemann, J., Sottrup-Jensen, L., and Thogersen, H. C. (1996) *J. Biol. Chem. 271*, 12909−12912.
19. Huang, W., Dolmer, K., Liao, X. B., and Gettins, P. G. W. (1998) *Protein Sci. 7*, 2602−2612.
20. Davis, C. G., Goldstein, J. C., Sudhof, T. C., Anderson, R. G. W., Russell, D. W., and Brown, M. S. (1987) *Nature 326*, 760−765.
21. Mikhailenko, I., Considine, W., Argraves, K. M., Loukinov, D., Hyman, B. T., and Strickland, D. K. (1999) *J. Cell Sci. 112*, 3269−3281.
22. Jeon, H., Meng, W., Takagi, J., Eck, M. J., Springer, T. A., and Blacklow, S. C. (2001) *Nat. Struct. Biol. 8*, 499−504.
23. Springer, T. A. (1998) *J. Mol. Biol. 283*, 837−862.
24. Herz, J. (2001) *Nat. Struct. Biol. 8*, 476−478.
25. Blacklow, S. C., and Kim, P. S. (1996) *Nat. Struct. Biol. 3*, 758−761.
26. Goldstein, J. L., Hobbs, H. H., and Brown, M. S. (1995) in *The metabolic and molecular bases of inherited disease* (Scriver, C. R., Beaudet, A. L., Sly, W. S., and Valle, D., Eds.) pp 1981−2030, McGraw-Hill, New York.
27. Nicholls, A., Sharp, K. A., and Honig, B. (1991) *Proteins 11*, 281−296.

BI015688M